Carbon Dioxide Mixtures as Working Fluid for High-Temperature Heat Recovery: A Thermodynamic Comparison with Transcritical Organic Rankine Cycles

Abubakr Ayub [1] , **Costante M. Invernizzi** [1,*] , **Gioele Di Marcoberardino** [1] , **Paolo Iora** [1] and **Giampaolo Manzolini** [2]

[1] Department of Mechanical and Industrial Engineering, University of Brescia, via Branze, 38, 25123 Brescia, Italy; a.ayub@unibs.it (A.A.); gioele.dimarcoberardino@unibs.it (G.D.M.); paolo.iora@unibs.it (P.I.)
[2] Energy Department, Politecnico di Milano, 20156 Milan, Italy; giampaolo.manzolini@polimi.it
* Correspondence: costante.invernizzi@unibs.it; Tel.: +39-030-3715-569

Abstract: This study aims to provide a thermodynamic comparison between supercritical CO_2 cycles and ORC cycles utilizing flue gases as waste heat source. Moreover, the possibility of using CO_2 mixtures as working fluids in transcritical cycles to enhance the performance of the thermodynamic cycle is explored. ORCs operating with pure working fluids show higher cyclic thermal and total efficiencies compared to supercritical CO_2 cycles; thus, they represent a better option for high-temperature waste heat recovery provided that the thermal stability at a higher temperature has been assessed. Based on the improved global thermodynamic performance and good thermal stability of R134a, CO_2-R134a is investigated as an illustrative, promising working fluid mixture for transcritical power cycles. The results show that a total efficiency of 0.1476 is obtained for the CO_2-R134a mixture (0.3 mole fraction of R134a) at a maximum cycle pressure of 200 bars, which is 15.86% higher than the supercritical carbon dioxide cycle efficiency of 0.1274, obtained at the comparatively high maximum pressure of 300 bars. Steam cycles, owing to their larger number of required turbine stages and lower power output, did not prove to be a suitable option in this application.

1. Introduction

The increase of conversion efficiency and promotion of energy recovery represent two effective strategies for primary energy savings. In particular, energy recovery from waste industrial heat represents an interesting option which is currently widely accepted and applied where possible [1].

According to its temperature level, waste heat can be used in a wide range of applications: from heat sources for heat pumps in district heating systems [2] to its direct utilization for preheating air or for steam generation and finally for power production by thermodynamic cycles [3–5].

According to [6], the waste heat recovery potential in industry in the EU accounts for about 920 TW h, with Germany, Italy, France and UK contributing about 50% of the overall potential. Moreover, about 30% of the theoretical waste heat is available at temperatures higher than 270 °C.

Basically, high-temperature waste heat sources are available in refineries (from the process of fluid catalyst cracking, for example, at 700 to 800 °C), in cement plants (at temperatures from 300 to 500 °C) and in steel and glass manufactory processes.

The dust content of the available flue gases is highly variable, depending on the industrial process. For example, in flue gases from cement plants, the dust content may range from 30,000 to 90,000 mg Nm^{-3}.

The cement industry is one of the largest contributors to carbon dioxide emissions and is very energy-intensive: the production of one ton of cement requires an energy consumption of about 4–5 GJ, with an average emission value of 0.81 kg$_{CO_2}$/kg$_{cement}$ [7,8]. Therefore, it is certainly appropriate, necessary and useful to recover energy from flue gases of the cement industry for the production of electricity, given the high available temperatures.

Heat recovery from dusty flue gases, which sometimes also contain sulphur compounds—and are therefore potentially corrosive—is a challenging problem, but the correct materials and suitable technologies are currently available [9,10].

A second important aspect of the problem is the use of advanced high-efficiency thermal power thermodynamic engines. Usually, Rankine cycles with organic fluids are proposed, with good practical results [11–14]. The steam cycle is another well-known accepted possibility for energy recovery. In recent years, interest in trans-critical and supercritical thermodynamic cycles using carbon dioxide as a working fluid has grown. In [15], for example, a summary of proposals in the literature of carbon dioxide cycles for heat recovery from waste heat is presented. In [7], the authors report a literature overview of power cycles that were proposed for heat recovery in cement plants. The energy efficiencies of the thermodynamic cycles listed in the paper range between 11% and 30%, according to the temperature of the considered heat source (270 to 400 °C), the thermodynamic cycle and working fluid (organic fluids, steam or carbon dioxide).

With regard to carbon dioxide cycles, in [16], a good review of the main advantages and drawbacks of the use of carbon dioxide as a working fluid is presented. Briefly, one advantage is that a very high power density is produced due to the high pressure levels; furthermore, in the supercritical configuration, reasonably high cycle efficiencies even at moderate maximum temperatures can be achieved, but with the need of a large recuperator. However, a corrosive behavior at temperatures greater than 500 °C is exhibited, requiring the use of nickel alloys. About 10 ten testing facilities are operating today globally, and many studies investigating this process are underway.

On the other hand, as regards Rankine cycles operating with organic fluids, there are now at least 1500–2000 installed engines globally with a wide range of applications (geothermal, biomass, solar and heat recovery) and powers (from a few tens of kW to units of a few tens of MW).

According to the analysis developed in [17], carbon dioxide cycles represent a potentially more effective solution than ORC for heat source temperatures greater than 350 °C; this is particularly true if cold water is available, making condensation possible.

In the following, we consider as a case study the heat recovery from flue gases available at 450 °C (a typical maximum reference value for a cement plant) with a mass flow of 100 kg s^{-1}.

Usually, in a cement plant, two different hot gas streams are available (see, for example [7,11]): from kiln preheaters and from clinker coolers at different exhaust temperatures and with different exhaust mass flows. Here, for simplicity, we assumed the recovery of heat only from the flue gas flow at higher temperature.

Normally, an intermediate heat transfer fluid (diathermal oil or pressurised water) is interposed between the flue gas and the working fluid used in the thermodynamic cycle. Here, to simplify the scheme and the calculations, we considered a direct heat exchanger. On the other hand, some examples of direct heat exchangers are present in industrial practice.

Assuming a simple recuperative supercritical carbon dioxide cycle (the simplest plant configuration considered in literature) as a reference, we developed a performance comparison of transcritical ORC cycles with cycles adopting binary mixtures of carbon dioxide as a working fluid.

In addition to heat recovery, supercritical and transcritical carbon dioxide cycles have already been considered for a great variety of applications; for example, for solar plants, for nuclear power plants, for the exploitation of geothermal energy, and also for thermo-electric storage [18–21].

2. The Simple Recuperative Carbon Dioxide Cycle

In the thermodynamic exploitation of heat sources with a finite heat capacity, as in the case of hot flue gases, both the thermodynamic cycle efficiency and the effective cooling of the heat source are of paramount importance. This can be expressed, as is well known, by the total efficiency of a waste heat recovery system:

$$\eta = \frac{\dot{W}}{\dot{m}_H \left(H_{H_1} - H_{H_0}\right)} = \frac{\dot{W}}{\dot{m}_H \left(H_{H_1} - H_{H_2}\right)} \frac{H_{H_1} - H_{H_2}}{H_{H_1} - H_{H_0}} = \eta_{th}\phi \tag{1}$$

where η_{th} is the cycle's thermodynamic efficiency, ϕ is the heat recovery factor, and the enthalpy H_{H_0} represents the enthalpy corresponding to the minimum temperature T_{H_0} at which the flue gas can be cooled (see Table 1). In the following, to simplify the calculations and the general considerations, we assumed a value of T_{H_0} equal to the dew temperature of the flue gas.

Table 1. Design parameters assumed for the calculations.

Parameter	Assumed Value
Pressure losses	Neglected
Minimum internal temperature approach in the recuperator, $MITA_R$ (°C)	20
Minimum internal temperature approach in the primary heat exchanger, $MITA_{PHE}$ (°C)	50
Minimum internal temperature approach in the condenser, $MITA_C$ (°C)	20
Turbine efficiency, η_T	0.85
Compressor/pump efficiency, η_P	0.8
Mechanical efficiency of the compressor/pump	0.98
Mechanical/electrical efficiency of the turbine	0.95
Cooling air temperature (inlet T_{C_1}/outlet T_{C_2}) (°C)	15/35
Temperature of the available flue gas, T_{H_1} (°C)	450
Mass flow of the hot flue gas, $\dot{m}_H$ (kg s^{-1})	100
Composition of the flue gas (molar fractions)	N$_2$ 0.58; O$_2$ 0.03 CO$_2$ 0.28; H$_2$O 0.11
Dew temperature of the flue gas, T_{H_0} (°C)	51
Thermal power available in the flue gas, $\dot{m}_H \left(H_{H_1} - H_{H_0}\right)$ (MW)	44.06

Thus, for a fixed T_{H_1} and a mass flow $\dot{m}_H$ of flue gas, there is an optimal cycle maximum temperature and an optimal maximum cycle pressure that optimize the total efficiency η.

In fact, high maximum cycle temperatures T_3 and small expansion ratios $r_C = P_2/P_1$ result in a relatively high η_{th}, but a low ϕ. On the contrary, low values of T_3 and high values of r_C cause a low η_{th} and a high ϕ. Therefore, an optimal compromise between the maximum cycle temperature and the compression ratio must be identified.

In Table 1 the main design parameters assumed for all the following calculations are listed. In Figure 1, we show the considered plant scheme, with the compressor conceptually changed to a pump in all cycles with condensation. All the calculations are carried out with Aspen Plus® V9. The model used for all thermodynamic evaluations is the well known Peng–Robinson equation of state. An equation of state is generally considered for the evaluation of the volumetric properties of the real gases in thermodynamic and in fluid-dynamic calculations [22–24]

As an example, Figure 2 shows two carbon dioxide thermodynamic cycles at different T_3 and different r_C values. Cycle (a) has a maximum temperature of 350 °C and a compression ratio $r_C = 3.5$, while cycle (b) has $T_3 = 400$ °C and $r_C = 2$. The efficiency η_{th} of cycle (b) is slightly greater than the efficiency of cycle (a), but its lower ϕ (0.438 against about 0.6) appreciably detracts from the total efficiency η (0.097 versus 0.129).

In the following, we assumed a minimum pressure P_1 equal to 100 bar for carbon dioxide cycles, taking advantage of the cycle efficiency of the real gas effects in the compression phase [25].

Figure 3 presents the thermodynamic cycle efficiency and the total efficiency of simple recuperative carbon dioxide cycles. The temperature T_{H_1} of the flue gas was assumed to be equal to 450 °C (according to Table 1).
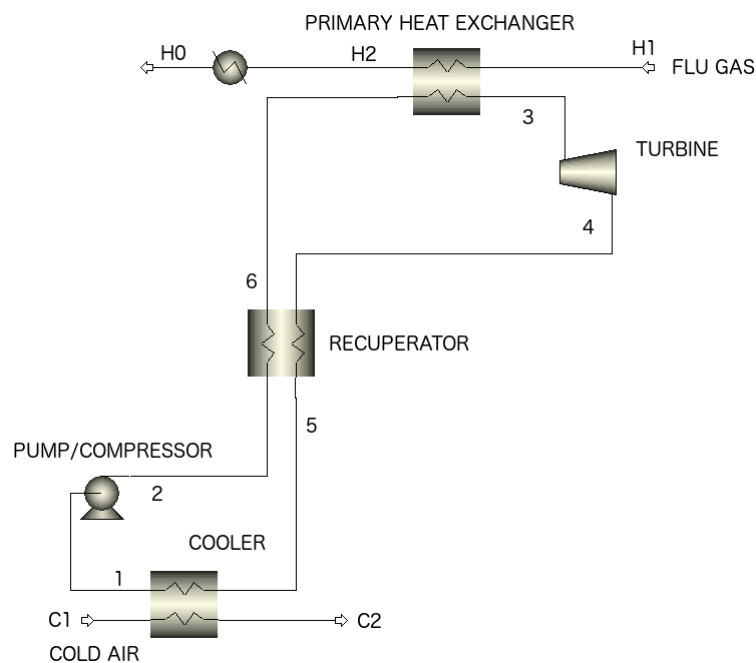

Figure 1. The reference plant scheme generally assumed for the calculations. The pump and the compressor are interchangeable depending on whether there is condensation. In some cases (according to the working fluid), the recuperator may not be necessary.
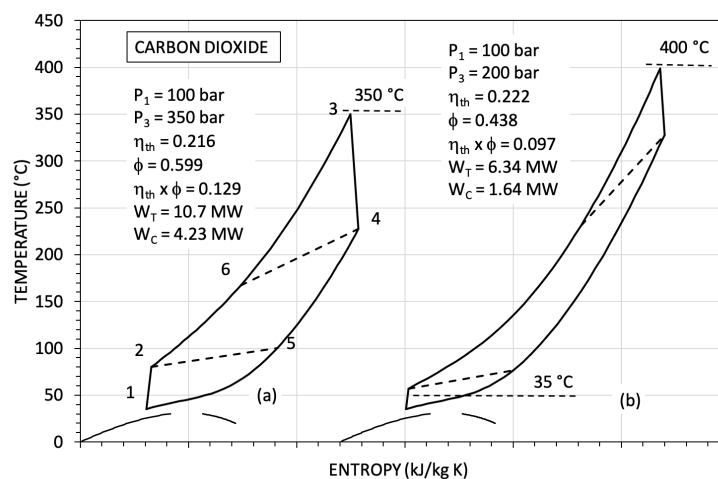

Figure 2. Simple recuperative carbon dioxide cycles in the T–S thermodynamic plane.

As the optimal maximum cycle temperature T_3 is equal to 350 °C, in the following, we assumed for simplicity the same value for all the considered working fluids and for all the discussed cases.

In Figure 4 cycle (a) of Figure 2 is reported in a plane of temperature–transferred power. In this plane, the relations between the thermodynamic cycle and the heat sources are shown. The maximum pressure of this cycle (350 bar) is not feasible in practical applications, although these conditions

correspond to the maximum value of η. In any case, the considerations of this case are also extended to cycles with different compression ratios.
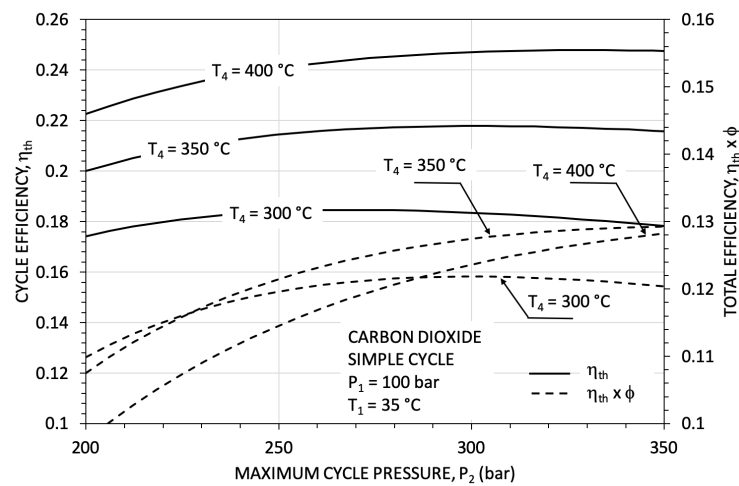

Figure 3. Thermodynamic cycle efficiency η_{th} and total efficiency $\eta = \eta th\phi$ as a function of the maximum cycle pressure for different maximum cycle temperatures T_4. The results are for simple recuperative supercritical carbon dioxide cycles.

The heat source is cooled from $T_{H_1} = 350\,°C$ to $T_{H_2} = 217\,°C$ ($\phi \approx 0.6$) and the remaining potentially available thermal energy (from T_{H_2} to $T_{H_0} \approx 51\,°C$) is lost. The transferred heat in the recuperator is about 2.5 times greater than the net power, and the air mass flow required at the radiator is almost 10 times that of the carbon dioxide circulating in the engine. The high power required by the ventilators could affect the system efficiency and the radiator—i.e., one of the major cycle components. The assumed constraint of an $MITA_C$ equal to $20\,°C$ results in a temperature T_1 of $35\,°C$ (corresponding to a reduced temperature T_r of 1.01).

These results seem consistent with those obtained in [15], considering that the authors assumed a maximum cycle pressure of 200 bar and a relatively high recuperator efficiency of 95% (five points higher than the efficiency resulting from the present analysis).
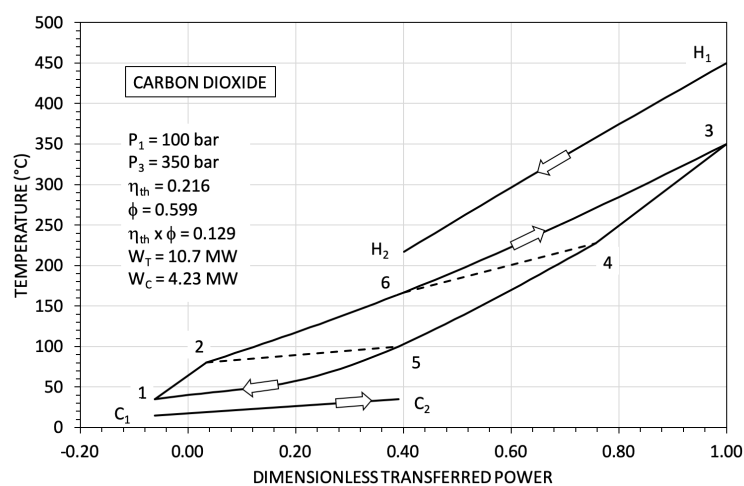

Figure 4. The simple carbon dioxide thermodynamic cycle shown in Figure 2 and the heat sources in a plane of temperature–dimensionless transferred power.

More advanced plant configurations (with a single split, a dual split and possibly with an intercooler) were not considered here. They performances and a detailed description of the plant

arrangements are described, for example, in [15,17,26]. In the following, we concentrate our attention on the transcritical Rankine cycles using organic fluids.

3. Recuperative Cycles with Organic Working Fluids

Dealing with heat sources with finite heat capacity, the total efficiency in Equation (1) can be optimized adopting an ideal "triangular" cycle. These conditions can be approximated by resorting to working fluids with a critical temperature close to that of the maximum heat source [27,28]. On the other hand, when the critical temperature of the working fluid is much lower than the maximum temperature of the heat source, the ideal thermodynamic cycle approaches the transcritical conditions.

In addition to an adequate critical temperature, another important parameter to consider in the selection of the working fluid is a relatively low molecular complexity to avoid superheating during the adiabatic expansion. Nonetheless, excessively low molecular complexity is still not recommended as it results in an adiabatic expansion in the two-phase region.

The molecular complexity of a working fluid can be quantified, for example, by the molecular complexity parameter $\sigma = \frac{T_c}{R} \left(dS/dT \right)_{T_r=0.7,dew}$ [29] (p. 109). In general, working fluids with $\sigma \approx 0$ show (for reasonable pressure expansion ratios and for a starting point corresponding to the saturated vapor) an adiabatic expansion ending near the upper limit curve (the dew line).

As the molecular complexity is strictly correlated to the isentropic exponent $(\gamma - 1)/\gamma$, working fluids with a small molecular complexity (a relatively large negative value of σ) experience a substantial cooling during an adiabatic expansion (with a fixed pressure expansion ratio [29]; see Section 2.5).

On the other hand, the molecular weight of the fluid directly affects the enthalpy variations: the higher the molecular weight, the lower the number of the turbine stages, and for a fixed input thermal power, the higher the mass low rate. Both if these results have positive effects on the component design.

According to the previous considerations, the fluids listed in Table 2 were chosen. Carbon dioxide is shown in the table as a reference. Water is extensively and successfully used in the traditional Rankine cycles in plants with a high power size (of hundreds of MW).

Refrigerant R-134a (1,1,1,2-tetrafluoroethane, CH_2FCF_3) is a well known refrigerant and together with propane represents a working fluid with a medium molecular complexity ($\sigma \approx -2$). Hydrogen sulphide has a critical temperature similar to that of R-134a and of propane, but it has a smaller molecular complexity ($\sigma \approx -7$); on the contrary, perfluorobutane represents a fluid with a relatively high molecular complexity ($\sigma \approx 13$). Ammonia and chloromethane have a similar critical temperature and similar molecular complexity.

Methanol and dichloromethane represent two fluids with the same critical temperature but with an appreciably different molecular complexity.

Table 2. Some thermodynamic data for the considered working fluids.

Fluid	Critical Temperature (°C)	Critical Pressure (bar)	Molecular Weight	Parameter of Molecular Complexity [a]	Isentropic Exponent [b]
Carbon dioxide	31.06	73.83	44.01	-	0.2232
Perfluorobutane	113.2	23.23	238.0	13.37	0.04524
R134a	101.0	40.56	102.0	−2.346	0.09730
Propane (R-290)	96.68	42.48	42.48	−2.409	0.1129
Water	373.9	220.6	18.01	−10.38	0.2476
Hydrogen sulphide	100.4	89.63	34.08	−7.416	0.2432
Ammonia	132.5	112.8	17.03	−9.231	0.2338
Chloromethane (R-40)	143.1	66.80	66.8	−7.115	0.2018
Dichloromethane (R-30)	236.8	60.8	84.93	−4.793	0.1622
Methanol	239.3	80.84	32.04	−10.63	0.1889

[a] $\sigma = \frac{T_c}{R} \left(dS/dT \right)_{T_r=0.7,dew}$, see [29] (p. 109). [b] $(\gamma - 1)/\gamma$ with $\gamma = C_P/C_V$ for ideal gas at 25 °C.

Obviously, not all of the fluids listed in Table 2 can actually be proposed as working fluids. For example, hydrogen sulphide is extremely toxic and flammable (see Table 3), while perfluorobutane has a high GWP.

All of the fluids in Table 2 were primarily selected to elucidate the impact of the main properties of the different fluids on the final thermodynamic performances of heat recovery Rankine cycles. Other fluids can be considered for more detailed and more specific analyses aimed at selecting the optimum working fluid.

Table 3. Some environmental and safety properties of the considered fluids.

Fluid	Toxicity [a]	Flammability [a]	Instability/Reactivity [a]	GWP [d]	ODP
Carbon dioxide	2, SA [b]	0	0	1	0
Perfluorobutane	1	0	0	8600	0
R134a	1	0	1	1370	0
Propane (R-290)	2	4	0	≈20	0
Water	0	0	0	0	0
Hydrogen sulphide	4	4	0	na	na
Ammonia	3, COR [c]	1	0	1	0
Chloromethane (R-40)	2	4	0	13	0.02
Dichloromethane (R-30)	2	1	0	10	
Methanol	1	3	0	3	na

[a] according to NFPA 704, Standard System for the Identification of the Hazards of Materials for Emergency Response, https://www.nfpa.org/codes-and-standards/all-codes-and-standards/list-of-codes-and-standards/detail?code=704 . Toxicity 0–4, Flammability 0–4, Instability/Reactivity 0–4. For a concise codes description, see https://en.wikipedia.org/wiki/NFPA_704 NFPA 704 Codes. [b] Asphyxiant gas. [c] Corrosive. [d] over a 100 year period.

Another primary and decisive property that must be taken into account in the selection of the correct working fluid is its thermochemical stability at the devised maximum working temperatures.

Assessing the long-term thermochemical stability of a compound is generally very difficult to achieve, given the several variables involved and the different possible operating conditions: the metallic surfaces and their surface/volume ratio, the presence of contaminants, the final acceptable level of decomposition and the corrosion problems.

As an example, dichloro-methane (methylene chloride) in a quartz vessel starts to decompose at 450 °C and according to a sigmoid curve, after a reaction period of about 350 min, the decomposition reaches a maximum value of about 34% [30]. In a stainless steel (AISI 430F) cylinder, an appreciable decomposition starts at 350 °C [31]. Thus, in general, the presence of different materials and contaminants (air, water, oil) has a strong catalytic effect on the decomposition of the working fluid.

However, as the thermochemical stability is strictly correlated to the chemical stability (at least in an inert environment), we take carbon dioxide (a compound with a well established high chemical stability) as a reference; in Figure 5, values of the ratio $\Delta H_B = \Delta_f H^0 / n_B$ are reported as a function of the number of chemical bonds in the molecule n_B. As the standard enthalpy of formation, $\Delta_f H^0$ is proportional to the energy required/released during the formation of the molecule, while the parameter ΔH_B may be a rough indicator of the relative thermal stability of any working fluid.

Certainly, the thermochemical decomposition of a fluid occurs through many complex reactions and—as in all chemical reactions—the activation energy plays an important role. Thus, compounds that are apparently chemically unstable (with a positive $\Delta_f H^0$) can nevertheless show an acceptable chemical and thermochemical stability. Even so, the parameter ΔH_B can give an approximate useful indication for the first classification of working fluids. In Figure 5, all flammable compounds have a value of ΔH_B close to zero.
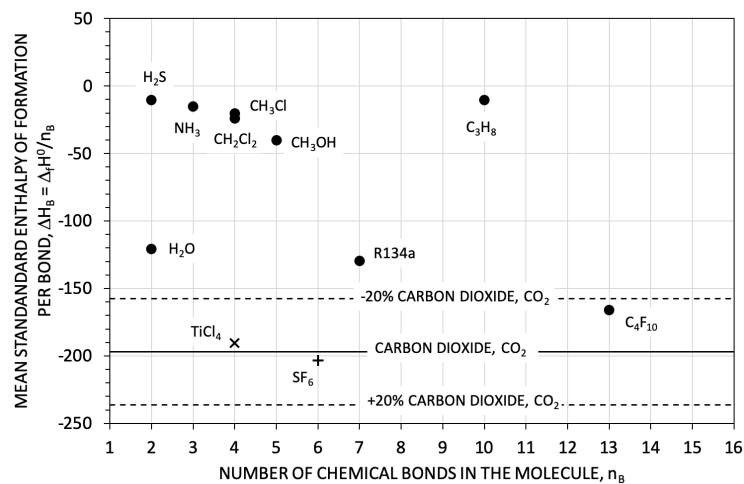
Figure 5. Mean standard enthalpy of formation per bond as a function of the bond number in a molecule for some different compounds. The values of $\Delta_f H^0$ are taken from [32] and from the data bank of [33].

Titanium tetrachloride $TiCl_4$ and sulfur hexafluoride SF_6 are also reported in Figure 5. Titanium tetrachloride is a compound that is considered as a possible working fluid in Rankine cycles at high temperatures, as it is industrially produced according a well known process at 700 to 1000 °C [34–36]. Sulfur hexafluoride is considered to be thermally very stable at least up to 400 to 600 °C [37] (p. 30).

In the following, for all the Rankine cycles, we assumed a maximum temperature T_3 of 350 °C, which represents a good compromise between the thermal stability limit for organic compounds and a reasonably good heat recovery factor.

Figure 6 reports the thermodynamic performances of the Rankine cycles operating with all the working fluids considered here.

The considered steam cycle is a standard superheated cycle (at temperature T_3), without feedwater heaters but with a deaerating heater at 5 bar. In the case of steam, a maximum total efficiency η of about 0.15 is reached at the evaporation pressure of 20 bar, with a turbine expansion ratio $r_T = r_T = P_3/P_1$ of 146.

Refrigerant R134a and propane have approximately the same global performance, and perfluoro-butane performs worse.
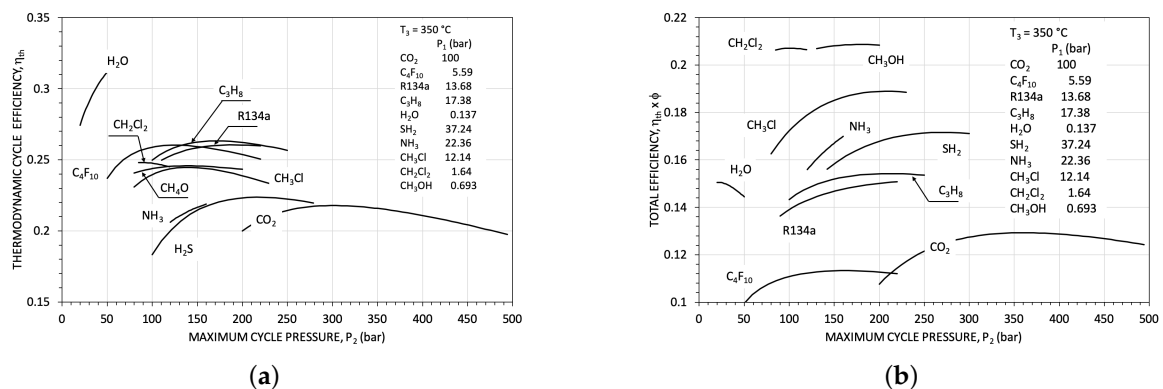

Figure 6. Cycle thermodynamic efficiency and total efficiency as a function of the maximum cycle pressure for all the considered working fluids: (**a**) cycle efficiency, (**b**) total efficiency.

The best performances in terms of total efficiency are obtained by dichloro-methane and methanol. In Figure 7, two cycles with dichloro-methane and methanol are reported in the T–S thermodynamic

plane, respectively. Thanks to the small molecular complexity, both fluids do not require a recuperator, and the heat recovery factor is therefore very high. The two cycles show basically the same thermodynamic performance, but the smaller σ parameter for methanol yields a final expansion in the two-phase region (with a vapor quality of about 0.9).
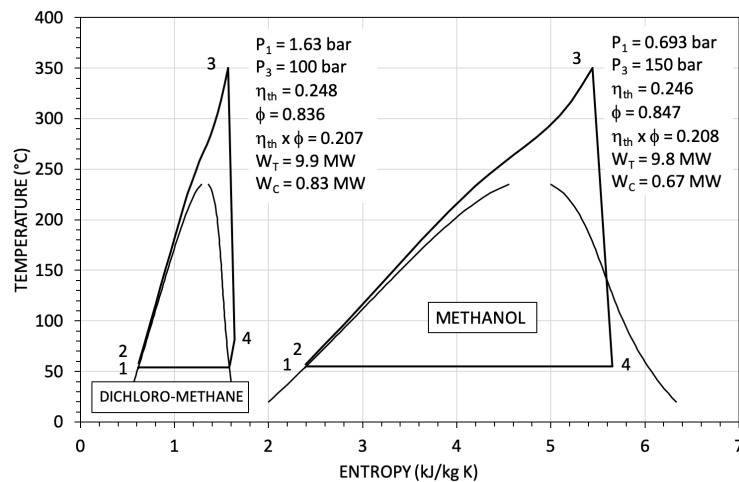

Figure 7. Thermodynamic cycles with dichloro-methane and with methanol in the T-S thermodynamic plane.

In Figure 8, cycles operating with dichloro-methane and perfluoro-butane in optimized conditions are presented in the temperature–dimensionless transferred power plane. The high molecular complexity of perfluoro-butane ($\sigma \approx 13$) produces a reduced cooling of the vapor during the expansion, requiring the use of a large recuperator ($\dot{Q}_R/\dot{W}_T = 4.7$). As a consequence, T_{H_2} is relatively high (285.34 °C) and ϕ is rather low (0.428). This result again supports the general thermodynamic convenience of resorting to working fluids with a low molecular complexity to recover energy from waste heat resources, unless the residual heat can be used for different purposes; for example, to preheat combustion air.
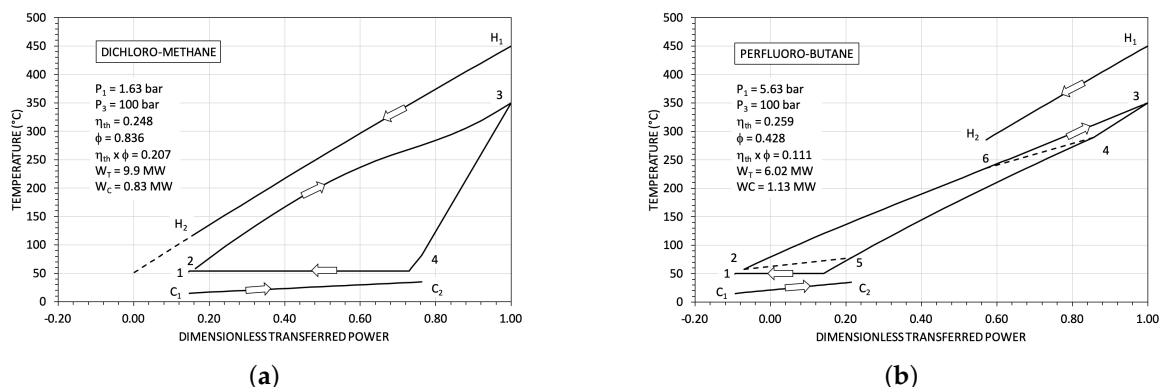

Figure 8. Two Rankine cycles with different working fluids in the plane of temperature–dimensionless transferred power: (**a**) dichloro-methane, (**b**) perfluoro-butane.

In this application, considering its global performance, environmental properties in Table 3 and predictably good thermal stability (see Figure 5), the refrigerant R134a seems to represent the best compromise among all of the potential different working fluids considered here.

Therefore, in the following section, the thermodynamic performances of mixtures of R134a and carbon dioxide will be investigated.

4. Transcritical Cycles with Mixtures of Carbon Dioxide

It is possible to vary the critical point of the resulting mixture of two fluids in different proportions and consequently alter its thermodynamic and thermophysical properties. Therefore, it is possible—at least in principle—to find the correct working fluid for any application [25]. For example, it is possible to produce condensation in hot environments or to control the pressure expansion ratio or the minimum and maximum pressures [38–41]. In particular, mixtures of carbon dioxide as working fluids in closed power cycles have already been considered by some authors in the past [42–45].

Figure 9a shows the pressure–temperature (P–T) envelopes for different mixtures of carbon dioxide (component 1) and propane (component 2) evaluated by Aspen Plus® V9. The critical locus is calculated by a code based on the approach described in [46], where the Peng–Robinson equation of state in its simpler and original formulation has been implemented [47] (pp. 208, 423). The experimental points available in the data bank of Aspen Plus® V9 are reported for comparison. The developed code is capable of computing both stable and metastable critical points at given composition of any binary mixture without any initial estimation.

In Figure 9b, we present the P–T envelopes and critical loci for mixtures of carbon dioxide and the refrigerant R134a. With the composition of the mixture, the critical temperature and the critical pressures change continuously from that of pure carbon dioxide ($z_1 = 1.0$) to that of pure R134a ($z_1 = 0.0$). At $z_1 = 0.7$, the critical temperature is about $60\,°C$ and the critical pressure is $70\,bar$, thus allowing condensation with a bubble temperature of $35\,°C$.

Figure 10a,b shows values of the thermodynamic cycle efficiency η_{th} and of the total efficiency $\eta = \eta_{th}\phi$ as a function of the maximum cycle pressure, respectively, for mixtures of carbon dioxide and R134a.
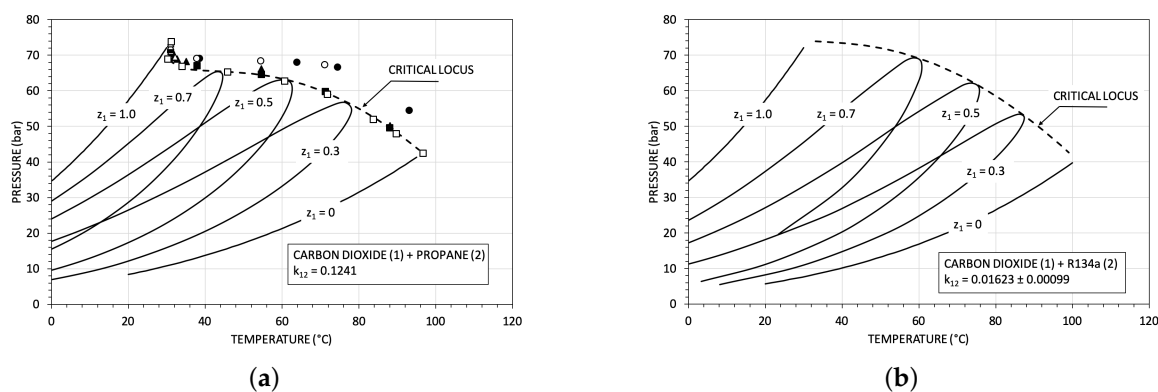

Figure 9. Pressure–temperature (P–T) envelopes and critical loci for mixtures of carbon dioxide. The symbols represent experimental points from different data sets in Aspen Plus® V9. (**a**) Carbon and propane. (**b**) Carbon dioxide and refrigerant R134a.

The mixture corresponding to $z_1 = 0.7$, at $P_3 = 200\,bar$ yields an η equal to 0.143—a value only slightly lower than the optimum value for the pure R134a (0.15), but with a halved expansion ratio, as shown in Figure 11. On the other hand, a carbon dioxide cycle with a maximum pressure of 200 bar has a total efficiency of only 0.107.
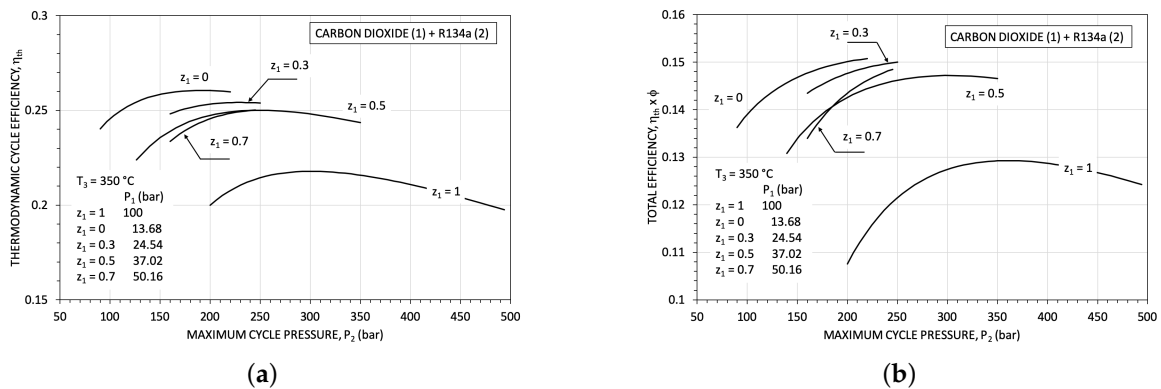
Figure 10. Cycle thermodynamic efficiency (**a**) and total efficiency (**b**) for some mixtures of carbon dioxide (component 1) and refrigerant R1234a (component 2). The compositions are expressed as molar fractions of carbon dioxide.
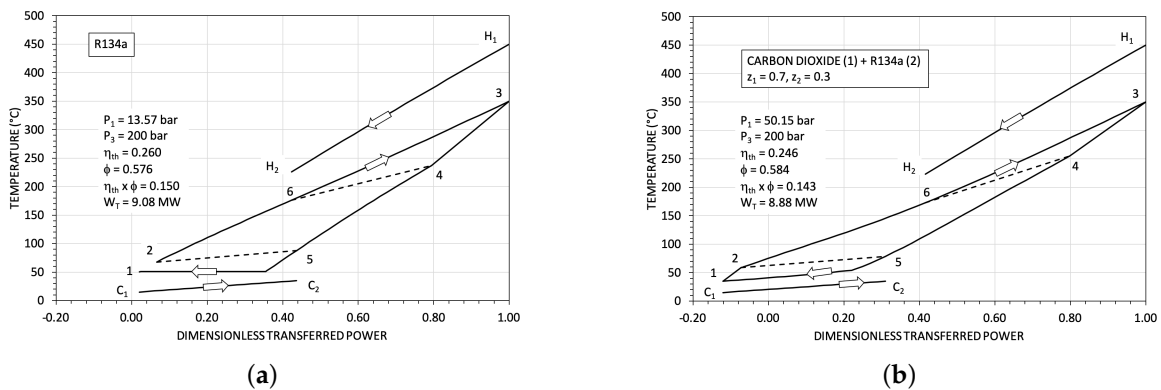

Figure 11. Thermodynamic cycles with (**a**) pure R134a; (**b**) a mixture of carbon dioxide ($z_1 = 0.7$) and R134a ($z_2 = 0.3$).

Table 4 summarizes the supercritical cycles with pure carbon dioxide, pure R134a and a mixture of carbon dioxide/R134a. The results for steam are also included for comparison.

The cycle with pure carbon dioxide at $P_3 = 250$ bar has a total efficiency η of 0.1215; using pure R134a, we obtain a higher value of η of about 23% (0.15) but with a volume flow ratio of about 11.5 (5.8 times greater than that of the carbon dioxide cycle). The size parameter SP for R134a is greater and this, for the turbine design, represents a slight advantage. The isentropic turbine enthalpy drop, in both cases, is not very high (probably one axial turbine stage could be adequate) and the corresponding isentropic powers fo the turbines are about 10 MW in both cases.

The steam has a good performance ($\eta = 0.15$), but compared to R134a and pure carbon dioxide, it results in a rather complex turbine: the expansion has to be divided into two groups (high-pressure (HP) and low-pressure (LP)), with a total volume flow ratio (VFR) of about 68 and a rather low total power of about 7 MW. For this power size, the assumed efficiencies of the steam turbomachinery (0.85 for the turbine and 0.8 for the pump, see Table 1) are probably too optimistic. Furthermore, the high isentropic enthalpy drops require more stages (roughly 6–10 axial stages). These drawbacks negatively impact the steam cycle in the considered case.

The selected mixture represents a good compromise between the simple cycle with carbon dioxide and the cycle with pure R134a, with good thermodynamic efficiency, a rather small turbine enthalpy drop and a reasonable volume flow ratio.

Moreover, the relatively low fraction of refrigerant in the mixture (30%) has the advantages of increasing the total efficiency with respect to the pure carbon dioxide cycle, with lower operating

pressures and, at the same time, with a limited quantity of refrigerant, which is an expensive fluid with a relatively high GWP.

A direct comparison with other literature results is difficult as comprehensive thermodynamic analyses of mixtures of carbon dioxide for the particular case here considered are not available. Furthermore, different authors assume different parameters and different cycle configurations, according to the specific application and to their particular sensitivity to the design parameters. Nevertheless, in [15], extensive results for recuperative carbon dioxide cycles with different layouts are presented, and for the more elaborate cycle configuration considered (an inter-cooled cycle with a dual split and a dual expansion), at a maximum cycle temperature of 400 °C, a total efficiency η of about 0.17–0.18 is reported. In [48], for example, with reference to a glass furnace, a total efficiency η of about 20% for a recovery organic Rankine engine is reported, but the authors assume a minimum cooling temperature for the flue gas equal to 180 °C.

Obviously, other fluids can be considered as dopants for carbon dioxide (for example, hydrocarbons, some of the new available refrigerants or some of the new technical fluids that are commercially available). In any case, the thermodynamic evaluations require the use of suitable equations of state and, in general, the knowledge of the so-called binary interaction parameters. In the case of the well known Peng–Robinson equation of state, for example, the binary interaction parameters of a mixture $k_{i,j}$ are correlated to the intermolecular interactions between the different molecule pairs of the different molecules composing the mixture. For a mixture of two components, only one binary interaction parameter is necessary, typically identified by the symbol $k_{1,2}$.

The correct value of $k_{1,2}$ is usually calculated by a regression of the experimental VLE. Then, the coefficient a_{mix} b_{mix} of the equation of state for the specific mixture can be defined, for example, by the well known classical van der Waals formulation [47,49] (p. 423):

$$a_{mix} = z_1^2 a_1 + z_1 z_2 a_{1,2} + z_2^2 a_2 \tag{2}$$

$$b_{mix} = z_1 b_1 + z_2 b_2 \tag{3}$$

where a_i and b_i are the parameters for the pure components and

$$a_{1,2} = \sqrt{a_1 a_2}\,(1 - k_{1,2}) \tag{4}$$

In Figure 12, for 19 different mixtures of carbon dioxide, the values of the parameter $a_{1,2} = \sqrt{a_2}\,(1 - k_{1,2})$ are reported as a function of a_2. The coefficient a_2 is the specific coefficient relative to the second compound of the mixture according the van der Waals equation of state (with a_1, the constant coefficient for carbon dioxide) [50]:

$$a_2 = \frac{27}{64}\frac{\tau_{c,2}^2}{P_{c,2}} \tag{5}$$

$$\tau_{c,2} = k_B T_{c,2} \tag{6}$$

$$k_B = \frac{R}{N_A} \tag{7}$$

where, N_A is the Avogadro number, $R = 8.3143\,\mathrm{J\,mol^{-1}\,K^{-1}}$ is the gas constant and T_c and P_c are the critical temperature and the critical pressure, respectively.

The correlation in Figure 12 can be used for a first estimation of the binary coefficient parameter $k_{1,2}$ (the Peng–Robinson binary interaction parameter) for binary mixtures of carbon dioxide in case no experimental VLE data are available, thus allowing preliminary calculations of the performances of thermodynamic cycles. Nonetheless, experimental VLE values are obviously preferable.

Table 4. Some results for carbon dioxide in Rankine and transcritical mixture cycles. The maximum temperature T_3 was assumed to be equal to 350 °C for all the listed cycles.

	Working Fluid	P_3 [a] (bar)	P_1 [b] (bar)	η [c]	ΔH_S [d] (kJ kg^{-1})	VFR [e]	SP [f] (m)	$\dot{m}_{wf}$ [g] (kg s^{-1})	$\dot{m}_C$ [h] (kg s^{-1})
Supercritical Cycle	CO_2	200	100	0.1075	74.63	1.687	0.06399	115.00	912.9
	CO_2	250	100	0.1215	96.06	1.970	0.05638	107.8	939.3
	CO_2	300	100	0.1274	112.7	2.221	0.05154	103.0	962.1
Transcritical Cycles	Steam	20	0.1375	0.1504	328.0 [j] 569.3 [k]	2.904 [j] 23.42 [k]	0.08152 [j] 0.3138 [k]	9.491	853.6
	R134a	200	13.57	0.1501	112.7	11.48	0.08880	94.72	905.3
	CO_2 (0.7) / R134a (0.3) [i]	200	24.54	0.1476	108.6	6.344	0.07412	96.50	925.2

[a] Maximum cycle pressure. [b] Minimum cycle pressure. [c] Total efficiency. [d] Isentropic turbine enthalpy drop. [e] Isentropic turbine volume flow ratio ($VFR = \frac{\dot{V}_{out,S}}{\dot{V}_{in}}$) [51].

[f] Size parameter ($SP = \frac{\sqrt{\dot{V}_{out,S}}}{\Delta H_S^{0.25}}$) [51]. [g] Working fluid mass flow rate. [h] Cooling air mass flow rate. [i] Molar composition. [j] High-pressure turbine. [k] Low-pressure turbine.
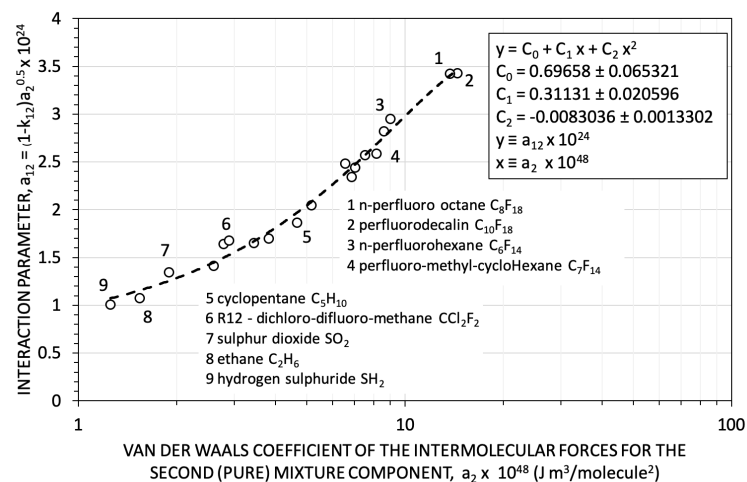
Figure 12. Binary interaction for different binary mixtures of carbon dioxide. The symbols correspond to the value of $k_{1,2}$ for the Peng–Robinson equation of state, regressed on experimental data, as available in the literature.

5. Conclusions

This study focused on the analysis of carbon dioxide mixture working fluids as an alternative to organic fluids, steam and pure carbon dioxide for high-temperature heat recovery in power plants. In order to explore this concept, a comparative analysis was carried out with transcritical Rankine cycles with organic working fluids, a standard superheated steam cycle, supercritical carbon dioxide cycle and transcritical cycles operating with carbon dioxide mixtures. Flue gases at a temperature of $450\,°C$ and a mass flow of $100\,kg\,s^{-1}$ were employed as the heat source for all thermodynamic cycles.

For Rankine cycles, a high critical temperature, low value of molecular complexity and high molecular weight were the three important prerequisites considered in this study for the choice of the working fluids. Therefore, eight working fluids including both lower and higher values of molecular complexity were considered to evaluate the effect of variations in fluid properties on cycle expansion ratios, heat transfer in recuperators, cycle thermal efficiency and total efficiency.

Salient points resulting from this study are summarized as follows:

- In simple recuperative carbon dioxide cycles, the total efficiency is improved by a comparatively high expansion ratio and low maximum temperature. The opposite occurs in the case of cycle thermodynamic efficiency. However, as a general rule, simple carbon dioxide cycles are ineffective at recovering heat, unless a high fraction of the residual heat in the source could be used in other ways (to preheat combustion air, for example).

- The results of Rankine cycles with pure organic working fluids show that the heat recovery efficiencies are remarkably better than those of the simple supercritical carbon dioxide power cycles. In relation to the considered specific application, working fluids with a low molecular complexity are to be preferred.

- Based on its acceptable global thermodynamic performance and presumably good thermal stability, R134a is investigated as an example of a dopant for the design of carbon dioxide mixtures. Thus, the critical points and P–T envelopes of CO_2-R134a mixtures were calculated at different molar compositions, which helped us to determine the composition of the mixture at the designed condensation temperature and pressure.

- A transcritical power cycle operating with CO_2-R134a mixtures showed an appreciable increase in cycle efficiencies as compared to simple supercritical carbon dioxide cycles at all maximum cycle pressures. In the case of the CO_2-R134a mixture corresponding to the 0.3 mole fraction of R134a, a total efficiency of about 0.15 was obtained at a maximum cycle pressure of $200\,bar$, compared to

the simple supercritical carbon dioxide cycle which presented a total efficiency of 0.12 at the same maximum pressure.

- Moreover, in comparison with pure R134a Rankine cycles, the transcritical cycle with a CO_2-R134a mixture (0.3 mole fraction of R134a) yielded the same total efficiency but with almost half the expansion ratio.

In summary, the transcritical cycle with the CO_2-R134a mixture (0.3 mole fraction of R134a) showed a good compromise between the simple R134a Rankine cycle and simple supercritical carbon dioxide cycles due to its good thermodynamic efficiencies, lower maximum operating pressures, lower expansion enthalpy drop and reasonable turbine volume flow ratios.

The standard enthalpy of formation per bond is proposed as a rough indicator of the thermal stability of the considered working fluids with reference to pure carbon dioxide; furthermore, a correlation to estimate the binary interaction parameters for carbon dioxide binary mixtures for which experimental VLE data are not available is suggested. This allows the calculation of thermodynamic properties, critical points and P–T envelopes of some new carbon dioxide mixtures and preliminary calculations of the thermodynamic performance of cycles. In this way, is it possible to analyze a broad spectrum of carbon dioxide mixtures to select the most promising components and—only after this preliminary analysis—to carry out the necessary experimental liquid–vapor measurements.

As in all transcritical and supercritical power cycles, the efficiency of the recuperator plays an important role, as the recovered heat is generally very high. For example, the ratio $\dot{Q}_R/\dot{W}$ is about 4.5 for simple supercritical carbon dioxide cycles at a maximum pressure of 250 bar and about 2.9 for the mixture CO_2 (0.7)-R134a (0.3).

The use of mixture of carbon dioxide in transcritical power cycles seems a promising solution to obtain (i) reasonable global efficiencies at a reasonable maximum pressure and (ii) with a conceptually simple plant configuration. On the other hand, points to investigate for a better design of the engine are (i) the vapour–liquid equilibria at different temperatures and pressures and, given the important role of the heat exchangers and of the turbomachines, (ii) the main transport properties (viscosity and thermal conductivity) of the most promising mixtures—properties that, for mixtures, are not simple to estimate properly for all of the relevant thermodynamic conditions.

Abbreviations

The following abbreviations, symbols and subscripts are used in this manuscript:

C_P	Heat capacity at constant pressure ($\mathrm{kJ\,kg^{-1}\,K^{-1}}$)
C_V	Heat capacity at constant specific volume ($\mathrm{kJ\,kg^{-1}\,K^{-1}}$)
$\dot{m}_H$	Mass flow rate of the flu gas ($\mathrm{kg\,s^{-1}}$)
$MITA_R$	Minimum Internal Temperature Approach in the recuperator (°C)
$MITA_{PHE}$	Minimum Internal Temperature Approach in the primary heat exchanger (°C)
$MITA_C$	Minimum Internal Temperature Approach in the radiator/condenser (°C)
P_C	Condensation pressure (bar)
P_c	Critical pressure (bar)
$\dot{Q}_R$	Recovered thermal power in the recuperator (kW)
R	Gas constant ($\mathrm{kJ\,kg^{-1}\,K^{-1}}$)
r_C	Compression ratio (P_2/P_1)
r_T	Expansion ratio (P_3/P_4)

S	Entropy (kJ kg^{-1} K^{-1})
SP	Size parameter for a stage of axial turbine $\left(\dot{V}_{out,S}^{0.5}/\Delta H_S^{0.25} \right)$
T	Temperature (°C or K)
T_{H_1}	Maximum temperature of the heat source (thermal oil) (°C or K)
T_c	Critical temperature (°C or K)
T_r	Reduced temperature ($= T/T_c$)
T_{C_1}	Cooling air inlet temperature (°C or K)
T_{C_2}	Cooling air outlet temperature (°C or K)
$\dot{V}$	Volumetric flow rate (m^3 s^{-1})
VFR	Isentropic flow ratio ($= \dot{V}_{out,S}/\dot{V}_{in} = \rho_{in}/\rho_{out}$)
$\dot{W}$	Mechanical or electrical power (kW)
$\dot{W}_S$	Isentropic power (kW)
z	Molar fraction
γ	Specific heat ratio (C_P/C_V)
ΔH_S	Isentropic turbine work (kJ kg^{-1})
η	Total efficiency ($\eta_{th}\phi$)
η_T	Turbine efficiency
η_{th}	Thermodynamic efficiency
η_P	Pump/compressor efficiency
ϕ	Heat recovery factor (see Equation (1))
σ	Parameter of molecular complexity $\left(= \frac{T_c}{R} \left[\frac{dS_{sv}}{dT} \right]_{T_r=0.7,dew} \right)$
HP	High pressure
LP	Low pressure
out	Outlet conditions
S	Isentropic conditions
1, 2, 3 …	Numbers identifying different points in the thermodynamic cycles

References

1. Santarossa, S. *Putting industrial waste heat to use*. Turboden: Brescia, Italy, 2018.
2. ReUseHeat Recovery of Urban Excess Heat, Horizon 2020 Project, Start Date: 1 October 2017, End Date: 30 September 2021, Grant Agreement 767429. Available online: https://www.reuseheat.eu (accessed on 6 June 2020).
3. TASIO, Waste Heat Recovery for Power Valorisation with Organic Rankine Cycle Technology in Energy Intensive Industries, Horizon 2020 Project, Start Date: 1 December 2014, End Date: 31 May 2019, Grant Agreement 637189. Available online: https://www.tasio-h2020.eu/ (accessed on 6 June 2020).
4. I-ThERM, Industrial Thermal Energy Recovery Conversion and Management, Horizon 2020 Project, Start Date: 1 October 2015, End Date: 30 June 2020, Grant Agreement 680599. Available online: http://www.itherm-project.eu (accessed on 6 June 2020).
5. Agathokleous, R.; Bianchi, G.; Panayiotou, G.; Arestia, L.; Argyrou, M.C.; Georgiou, G.S.; Tassou, S.A.; Jouhara, H.; Kalogirou, S.A.; Florides, G.A.; et al. Waste Heat Recovery in the EU industry and proposed new technologies. *Energy Procedia* **2019**, *161*, 489–496. [CrossRef]
6. Bianchi, G.; Panayiotou, G.P.; Aresti, L.; Kalogirou, S.A.; Florides, G.A.; Tsamos, K.; Tassou, S.A.; Christodoulides, P. Estimating the waste heat recovery in the European Union Industry. *Energy Ecol. Environ.* **2019**, *4*, 211–221. [CrossRef]
7. Kizilkan, O. Performance assessment of steam Rankine cycle and sCO$_2$ Brayton cycle for waste heat recovery in a cement plant: A comparative study for supercritical fluids. *Int. J. Energy Res.* **2020**, 1–15. https://doi.org/10.1002/er.5138 [CrossRef]
8. Worrel, E.; Price, L.; Martin, N.; Hendriks, C.; Meida, L.O. Carbon Dioxide Emissions from the Global Cement Industry. *Annu. Rev. Energy Environ.* **2001**, *26*, 303–329. [CrossRef]
9. Nimbalkar, S.U.; Thekdi, A.C.; Rogers, B.M.; Kafka, O.L.; Wenning, T.J. *Technological and Materials for Recovering Waste Heat in Harsh Environments*; ORNL/TM-2014/619; Oak Ridge National Laboratory: Oak Ridge, TN, USA, 2014.

10. Anonimous. *Corrosive Flue Gas Is No Longer a Show-Stopper for Heat Recovery*. Available online: https://heatmatrixgroup.com (accessed on 30 May 2020).

11. Santarossa, S. *Beating the heat*. Turboden: Brescia, Italy, 2020.

12. Lecompte, S.; Huisseune, H.; van der Broek, M.; Vanslambrouck, B.; De Paepe, M. Review of organic Rankine cycle (ORC) architectures for waste heat recovery. *Renew. Sustain. Energy Rev.* **2015**, *47*, 448–461. [CrossRef]

13. Macchi, E.; Astolfi, M. (Eds.) *Organic Rankine Cycle (ORC) Power Systems. Technologies and Applications*; Woodhead publishing: Duxford, UK, 2017; pp. 299–319.

14. Xu, W.; Zhao, Li, Mao, S.S.; Deng, S. Towards novel low temperature thermodynamic cycle: A critical review originated from organic Rankine cycle. *Appl. Energy* **2020**, *270*, 115186. [CrossRef]

15. Manente, G.; Fortuna, F.M. Supercritical CO_2 power cycles for waste heat recovery: A sistematic comparison between traditional and novel layouts with dual expansion. *Energy Convers. Manag.* **2019**, *197*, 111777. [CrossRef]

16. Marchionni, M.; Bianchi, G.; Tassou, S.A. Review of supercritical carbon dioxide (sCO_2) technologies for high-grade waste heat to power conversion. *SN Appl. Sci.* **2020**, *2*, 611. [CrossRef]

17. Astolfi, M.; Alfani, D.; Lasala, S.; Macchi, E. Comparison between ORC and CO_2 power systems for the exploitation of low-medium temperature heat sources. *Energy* **2018**, *171*, 1250–1261. [CrossRef]

18. Crespi, F.; Sánchez, D.; Rodriguez, J.M.; Gavagnin, G. A thermo-economic methodology to select sCO_2 power cycles for CSP applications. *Renew. Energy* **2018**, *147*, 2905–2912. [CrossRef]

19. Ahn, Y.; Bae, S.J.; Kim, M.; Cho, S.K.; Baik, S.; Lee, I.J.; Cha, J.E. Review of supercritical CO_2 power cycles technology and current status of research and development. *Nucl. Eng. Technol.* **2015**, *47*, 647–661. [CrossRef]

20. McDonnell, K.; Molnár, L.; Harty, M.; Murphy, F. Feasibility Study of Carbon Dioxide Plume Geothermal Systems in Germany—Utilising Carbon Dioxide for Energy. *Energies* **2020**, *13*, 2416. [CrossRef]

21. Ayachi, F.; Tauveron, N.; Tartière, T.; Colasson, S.; Nguyen, D. Thermo-Electric Energy Storage involving CO_2 transcritical cycles and ground heat storage. *Appl. Therm. Eng.* **2016**, *108*, 1418–1428. [CrossRef]

22. Matheis, J.; Müller, H.; Lenz, C.; Pfitzner, M.; Hickel, S. Volume translation methods for real-gas computational fluid dynamics simulations. *J. Supercrit. Fluids* **2016**, *107*, 422–432. [CrossRef]

23. Ziółkowski, P.; Badur, J.; Ziiółkowski, P.J. An energetic analysis of a gas turbine with regenerative heating using turbine extraction at intermediate pressure-Brayton cycle advanced according to Szewalski's idea. *Energy* **2019**, *185*, 763–786. [CrossRef]

24. Guardone, A. Nonclassical Gasdynamics: Thermodynamic Modelling and Numerical Simulation on Multidimensional Flows of BTZ Fluids. Ph.D. Thesis, Politecnico di Milano, Milan, Italy, 2001.

25. Invernizzi, C.M. Prospects of Mixtures as working Fluids in Real-Gas Brayton Cycles. *Energies* **2017**, *10*, 1649. [CrossRef]

26. Manente, G.; Costa, M. On the Conceptual Design of Novel Supercritical CO_2 Power Cycles for Waste Heat Recovery. *Energies* **2020**, *13*, 370. [CrossRef]

27. Invernizzi, C.; Bombarda, P. Thermodynamic performance of selected HCFS for geothermal applications. *Energy* **1997**, *22*, 887–895. [CrossRef]

28. Vivian, J.; Manente, G.; Lazzaretto, A. A general framework to select working fluid and configuration of ORCs for low-to-medium temperature heat sources. *Appl. Energy* **2015**, *156*, 727–746. [CrossRef]

29. Invernizzi, C.M. *Closed Power Cycles—Thermodynamic Fundamentals and Applications*; Springer-Verlag: London, UK, 2013.

30. Santacesaria, E.; Morini, A.; Carrá, S. Research on thermal decomposition of methylene chlorine. *La Chimica e l'Industria* **1974**, *56*, 74-753.

31. Santacesaria, E.; Morini, A.; Carrá, S. Influence of metallic surfaces on decomposition of methylene chlorine. *La Termotecnica* **1975**, *29*, 443–449.

32. Poling, B.E.; Prausnitz, J.M.; O'Connel, J.P. *The Properties of Gases and Liquids*, 5th ed.; McGraw-Hill: New York, NY, USA, 2001.

33. National Institute of Standard and Technology. US Department of Commerce. Available online: https://www.nist.gov (accessed on 12 June 2020).

34. Bombarda, P.; Invernizzi, C. Binary liquid metal-organic Rankine cycles for small power distributed high efficiency systems. *Proc. Inst. Mech. Eng. Part A J. Power Energy* **2015**, *229*, 1290–209. [CrossRef]

35. Invernizzi, C.M.; Iora, P.; Bonalumi, D.; Macchi, E.; Robert, R.; Caldera, M. Titanium tetrachloride as novel working fluid for high temperature Rankine cycles: Thermodynamic analysis and experimental assessment of the thermal stability. *Appl. Therm. Eng.* **2016**, *107*, 21–27. [CrossRef]

36. Bordbar, H.; Yousefi, A.A.; Abedini, H. Production of titanium tetrachloride ($TiCl_4$) from titanium ores: A review. *Polyolefins J.* **2017**, *4*, 149–173.

37. Anonymous. *Sulphur Hexafluoride*; Solvay Special Chemicals: Hannover, Germany. Available online: https://www.solvay.com/sites/g/files/srpend221/files/2018-08/SF6-Sulphur-Hexafluoride_0.pdf (accessed on 11 June 2020).

38. Invernizzi, C.M.; Iora, P. The exploitation of the physical exergy of liquid natural gas by closed power thermodynamic cycles. An overview. *Energy* **2016**, *105*, 2–15. [CrossRef]

39. Invernizzi, C.; Binotti, M.; Bombarda, P.; Di Marcoberardino, G.; Iora, P.; Manzolini, G. Water Mixtures as Working Fluids in Organic Rankine Cycles. *Energies* **2019**, *12*, 2629. [CrossRef]

40. Invernizzi, C.M.; Ayub, A.; Di Marcoberardino, G.; Iora, P. Pure and Hydrocarbon Binary Mixtures as Possible Alternatives Working Fluids to the Usual Organic Rankine Cycles Biomass Conversion Systems. *Energies* **2019**, *12*, 4140. [CrossRef]

41. Di Marcobeardino, G.; Invernizzi, C.M.; Ior, P.; Ayub, A.; Di Bona, D.; Chiesa, P.; Binotti, M. Experimental and analytical procedure for the characterization of innovative working fluids for power plants applications. *Appl. Therm. Eng.* **2020**, *178*, 115513. [CrossRef]

42. Jeong, W.S.; Lee, I.J.; Jeong, Y.H. Potential improvements of supercritical recompression CO_2 Brayton cycle by mixing other gases for power conversion system of a SFR. *Nucl. Eng. Des.* **2011**, *241*, 2128–2137. [CrossRef]

43. Invernizzi, C.M.; van der Stelt, T. Supercritical and real gas Brayton cycles operating with mixtures of carbon dioxide and hydrocarbons. *Proc. Inst. Mech. Eng. Part A J. Power Energy* **2012**, *226*, 682–693. [CrossRef]

44. Wright, S.A.; Pickard, P.S.; Vernon, M.E.; Radel, R.F. Enhancing Power Cycle Efficiency for a Supercritical Brayton Cycle Power System Using Tunable Supercritical Gas Mixtures. U.S. Patent No. 9,745,899, 7 February 2013.

45. Feng, L.; Zheng, D.; Chen, J.; Dai, X.; Shi, L. Exploration and Analysis of CO_2 + Hydrocarbon Mixtures as Working Fluids for Trans-critical ORC. *Energy Procedia* **2017**, *129*, 145–151. [CrossRef]

46. Michelsen, M.L.; Heidemann, A. Calculation of Critical Points from Cubic Two-Constant Equation of State. *Am. Inst. Chem. Eng. J.* **1981**, *27*, 521–523. [CrossRef]

47. Sandler, S.I. *Chemical, Biochemical, and Engineering Thermodynamics*, 4th ed.; John Wiley: New York, NY, USA, 2006.

48. Danieli, P.; Rech, S.; Lazzaretto, A. Supercritical CO2 and air Brayton-Joule versus ORC systems for heat recovery from glass furnaces: Performances and economic evaluation. *Energy* **2019**, *168*, 295–309. [CrossRef]

49. Kwak, T.Y.; Mansoori, G.A. Van der Waals mixing rules for cubic equations of state.Applications for supercritical fluid extraction modelling. *Chem. Eng. Sci.* **1986**, *41*, 1303–1309. [CrossRef]

50. Johnston, D.C. *Advances in Thermodynamics of the van der Waals Fluid*; IOP Publishing: Bristol, UK, 2014.

51. Macchi, E.; Astolfi, M. Axial flow turbines for Organic Rankine Cycles applications. In *Organic Rankine Cycle (ORC) Power Systems. Technologies and Applications*; Macchi, E., Astolfi, M., Eds.; Whoodhead Pubblishing: Duxford, UK, 2017.